

Environmental vs. demographic variability in two-species predator-prey models

Ulrich Dobramysl* and Uwe C. Täuber†

Department of Physics, Virginia Tech, Blacksburg, Virginia 24061-0435, USA

(Dated: August 1, 2021)

We investigate the competing effects and relative importance of intrinsic demographic and environmental variability on the evolutionary dynamics of a stochastic two-species Lotka-Volterra model by means of Monte Carlo simulations on a two-dimensional lattice. Individuals are assigned inheritable predation efficiencies; quenched randomness in the spatially varying reaction rates serves as environmental noise. We find that environmental variability enhances the population densities of both predators and prey while demographic variability leads to essentially neutral optimization.

PACS numbers: 87.23.Cc, 05.40.-a, 87.18.Tt

The mathematical modeling of species interactions continues to be a central issue in population ecology [1–4]. Several simple models have been proposed, investigated, and sometimes realized under laboratory conditions. Yet more realistic and thus biologically more relevant model variants obviously have to include both external spatial disorder in the reaction rates to account for varying environmental conditions and intrinsic demographic heterogeneity stemming from trait variability in individuals. While we addressed the former in a recent study [5], our goal in this letter is to investigate the interplay between quenched spatial rate disorder and *additional* variability of individuals’ reaction rates, as well as intriguing evolutionary co-optimization within interacting populations.

We focus on the Lotka-Volterra (LV) predator-prey model owing to its simplicity and because its basic features are well-understood. It was first introduced to study fish populations in the Adriatic sea and chemical oscillations [6, 7]. While the original deterministic LV (mean-field) equations yield neutral cycles and hence persistent nonlinear oscillations around a marginal fixed point [1], in stochastic implementations this species coexistence fixed point becomes stable and is approached very slowly through damped oscillations [8–14]. Spatially extended stochastic versions of the LV model yield striking dynamical patterns and emergent inter-species correlations [15–21] which may be utilized to quantitatively assess the response to external or internal changes. Population stability can be measured via the extinction time in small systems, where the stochastic kinetics ultimately reaches an absorbing zero-particle state [20, 22].

In our study of the effects of environmental rate variability in the LV model, we found a remarkable increase of the asymptotic population densities of *both* species with enhanced quenched spatial disorder, i.e., predation rates that are fixed to different lattice sites [5]. Yet the observed erratic population oscillations and relaxation towards the (quasi-)steady state occur on the time scale of many generations; for real biological systems, one therefore needs to address Darwinian evolutionary adaptation of individuals’ traits. Consequently, we introduce fundamentally novel features by endowing *in-*

dividual predator and prey particles with randomly selected rates, and investigate whether and how optimization within each species due to imperfect efficiency inheritance (mimicking random mutations) further reinforces the total population’s stability and fitness. Dynamical coevolution of interacting species is a crucial feature of adapting ecological systems and has been studied experimentally [23, 24] as well as theoretically [25–28]. Combining quenched spatial with individual, evolving rate distributions allows us to quantitatively assess the relative importance of environmental vs. demographic, inheritable variabilities in a nonlinear competing two-species predator-prey system.

We find that *both* environmental and individual-based variabilities combined with random mutations produce a marked enhancement of the quasi-stationary densities of both species, thus considerably extending our earlier conclusions for purely environmental randomness [5]. In addition, individual variability stabilizes both predator and populations against extinction. Remarkably, the optimization of predation and evasion capabilities of either species turns out to be essentially neutral in the population densities; in contrast to genetic drift models [29], our nonlinear model does not lead to trait fixation.

We consider a spatially extended version of the LV model consisting of two particles species. The “predator” species is subject to spontaneous decay $A \rightarrow \emptyset$ with rate μ , while the “prey” B reproduce (asexually): $B \rightarrow 2B$ with rate σ . Different particles interact on-site with a non-uniform predation rate λ , whereupon a prey is removed and replaced with a predator: $A + B \rightarrow 2A$. The prey birth and predator death rates both remain fixed at a uniform value $\sigma = \mu = 0.5$ for all particles and lattice sites, whereas the predation rates are allowed to vary between different positions and participating particles (see below). Particles exist on a two-dimensional square lattice with 128×128 sites and periodic boundary conditions. (We could not find significant finite-size effects already at this lattice size.) Both species perform unbiased random walks via nearest-neighbor hopping occurring with probability one, hence all rates are to be understood relative to the diffusivity D . Reactions occur

on-site, assuming infinite local carrying capacities, implying that the growth of the population on any single site is essentially unrestricted (with a safety limit of $n_i \leq 1000$ per lattice site i that is never reached with the parameters investigated in the present study). The predator extinction transition occurring in model variants with restricted site occupation is thus absent here [12, 20, 21]. The initial population distribution of both predator and prey particles is chosen randomly with a mean density $\rho_{A,i} = \rho_{B,i} = 1$. The simulation proceeds via random sequential updates, with one Monte Carlo step being completed when on average each particle in the simulation has moved and had a chance to react [30].

In order to model variability of individuals and trait inheritance, each particle carries a predation efficacy property $\eta \in [0, 1]$, determined during the particle's creation and providing a coarse-grained characterization of the combined efficacies of its genetic heritage (genes) and its learned strategies (memes). An offspring's position in efficiency space will thus be near its parent's location but subject to random changes (mutations in the case of genes, adaptations of strategies in the case of memes), thereby suggesting the use of a normalized Gaussian distribution centered at the parent's efficiency value η_P (truncated to the interval $[0, 1]$ accessible to a reaction probability) to assign an efficiency value η_O to the offspring during reproduction. The standard deviation w_P of the Gaussian function constitutes a model parameter and corresponds to the average severity of mutations from one generation to the next. Note that the efficiency assigned to a particle η is different from the traditional genetic fitness, which is defined as the average number of offspring produced by a genome. It represents a mesoscopic continuous stochastic variable, as opposed to a genetic description employing naturally discrete values.

Since we wish to address the distinctions between internal and spatial randomness, we introduce in addition environmental variability by assigning a spatial predation efficacy value η_S to each lattice site, drawn from a normalized Gaussian distribution with fixed mean 0.5 and standard deviation w_S , truncated to $[0, 1]$, and set to be fixed in time [31]. The ensuing predation rate λ is a random variable as well, namely a function of both the spatial efficiency at the lattice site the reaction occurs on and the two individual predation efficacies of the participating predator and prey particles. We finally define a model parameter ζ that describes the relative importance of the spatial over individual efficacies:

$$\lambda = \zeta \eta_S + (1 - \zeta) (\eta_A + \eta_B)/2. \quad (1)$$

Over many generations, species optimize their predation / evasion efficiency through evolving their efficacy distributions by means of random inheritance. Figure 1(a) shows the population density histograms $\rho_{A/B}(\eta)$ for a representative case with moderate inheritance variability $w_P = 0.1$. The initial population of

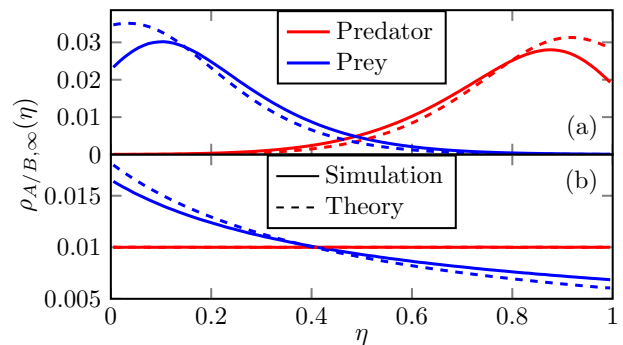


FIG. 1: (Color online.) (a) The predator (red) and prey (blue) population densities in the (quasi-)steady state as functions of the predation efficiency, averaged over 10^4 Monte Carlo simulation runs, optimize towards high $\bar{\eta}_A \approx 0.71$ and low $\bar{\eta}_B \approx 0.26$ mean values, respectively. The standard deviation of the Gaussian inheritance distribution is $w_P = 0.1$ and the spatial influence factor $\zeta = 0$. In contrast to genetic drift models, both densities do not fixate at extreme predation efficiencies ($\eta = 0, 1$). The dashed lines show the theoretical prediction from an effective stochastic mean-field model. (b) For a flat inheritance distribution ($w_P = \infty$), the predators experience no selection bias while the prey population is preferentially selected towards low predation efficacies.

predator and prey particles had an assigned predation efficacy of $\eta_{A/B} = 0.5$. We have carefully checked that the final (quasi-)steady state population distribution does not depend on the (uncorrelated) initial conditions (except for those rare simulation runs when either the prey or predator population went extinct). The predator population maximum moves towards higher mean efficacy whereas the prey population, for which lower values of the predation efficiency are preferable, tends towards a lower average. Predators with a slightly higher efficiency value are more successful at predation and thereby reproduce more often. Hence their improved predation capability is passed on to subsequent generations with a higher frequency, driving the overall predator population toward higher efficiency values. Similarly, prey particles with a lower predation efficiency are better at evasion and thus survive longer. This gives them the chance to reproduce at a higher rate, driving the prey population towards low mean efficacy. In the extreme situation of completely random assignment of predation efficiencies, where no correlations between the corresponding values for parents and offspring are implemented (equivalent to a uniform inheritance distribution with $w_P = \infty$), we already see a strong tendency towards low efficacies for the prey species; see Fig. 1(b). This feature is explained by the bias in the predation rule that favors selection of prey particles with higher efficiency values. For predators no such bias exists; hence their population distribution in efficiency space remains flat. Spatial fluctuations modify the results quantitatively, but not qualitatively, whence

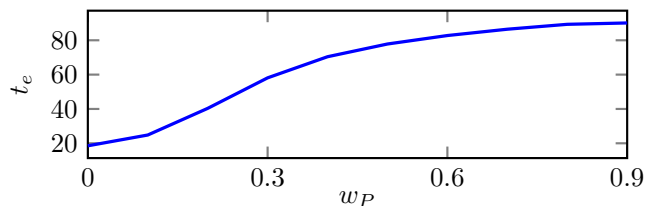


FIG. 2: (Color online.) Mean extinction time t_e of a small system of 10×10 lattice sites as a function of individual variability w_P and for $\zeta = 0$. Extinction here is defined as the event when either species goes extinct. With increasing variability the system on average takes longer to go extinct.

we observe a slightly more pronounced effect in the prey distribution in our studies of non-spatial systems.

In order to analytically verify our data we write down the mean-field equations for a well-mixed zero-dimensional LV system with individual variability. We consider the number of particles of species A and B as a function of predation efficiency. The predation efficiency η is a bounded quantity in the interval $[0, 1]$ assigned to particles at their time of creation. We discretize this interval into N bins with a spacing of $\Delta\eta = 1/N$ and midpoint $\eta_i = (i + 1/2)/N$, and denote the number of A and B particles in a bin i respectively as a_i and b_i ($i = 0, \dots, N - 1$). To model individual variability we introduce the probability $f_{ij} = f(\eta_i, \eta_j)$ for a parent with efficiency η_i to produce offspring with efficiency η_j . The predation rate is a function of the efficacies of the predator A and prey B participating in the predation reaction: $\lambda_{ij} = (\eta_i + \eta_j)/2$ [essentially the discretized Eq. (1) with $\zeta = 0$]. Thus we arrive at the coupled mean-field rate equations for the case of purely individual variability:

$$\dot{a}_i = -\mu a_i + \sum_j \sum_k \lambda_{jk} f_{ik} a_k b_j, \quad (2)$$

$$\dot{b}_i = \sigma \sum_k f_{ik} b_k - \sum_j \lambda_{ij} a_j b_i. \quad (3)$$

The steady-state densities are obtained by setting the time derivatives to zero, yielding expressions for a_i and b_i that can be solved iteratively for any inheritance probability distribution f , as shown (dashed) in Fig. 1(a).

In the special case of a uniform probability distribution (implying the absence of any correlation between the predation efficiencies of parent and offspring particles) $f_{ij} = 1/N$, the steady-state densities, defined by $\rho_{A,i} = a_i / \sum_j a_j$ and $\rho_{B,i} = b_i / \sum_j b_j$, can be obtained exactly. The predator population acquires a constant (η -independent) value of $\rho_A = 1/N$, whereas the prey population decreases with increasing η as $\rho_B(\eta) = \frac{2}{N \ln 3} \frac{1}{1+2\eta}$. This result is exactly mirrored by our zero-dimensional Monte Carlo simulations. In spatially extended systems fluctuations modify the density distributions, leading to a prey density dependence that is slightly less steep as a function of the predation efficiency, see Fig. 1(b). Correlation effects not captured by mean-field theory are evidently strongest at the distribution maxima.

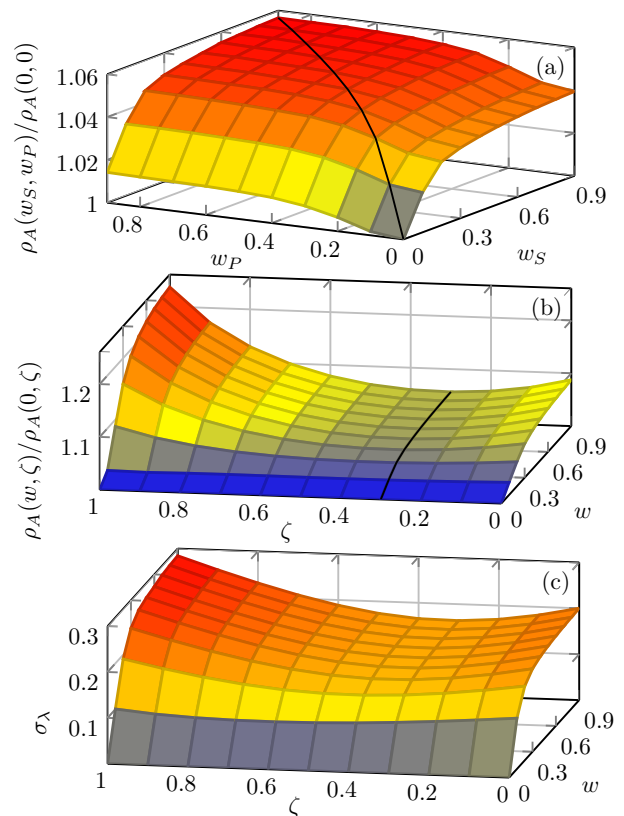


FIG. 3: (Color online.) (a) The (quasi-)steady state predator density ρ_A as a function of the spatial and individual variability w_S and w_P for $\zeta = 0.3$. The black line represents the slice of equal spatial and individual variability $w_S = w_P$ from the minimum in (b). (b) The predator density shows a consistent increase for all values of the spatial variability influence ζ as function of equal variabilities $w = w_S = w_P$ over a system with zero variability. A remarkable minimum is observed near $\zeta = 0.3$ (black line). (c) The standard deviation of the predation rate σ_λ , calculated via error propagation from the spatial and individual predation efficiency distributions.

We collected extinction time histograms for small systems (lattice size 10×10 sites) to determine the influence of individual variability on the stability of the population. In finite stochastic systems with an absorbing state (here, predator extinction), fluctuations will eventually drive the system into the absorbing state. Figure 2 demonstrates that the mean extinction time is enhanced by a factor up to ≈ 4.5 by individual variability, rendering the system markedly more robust against extinction.

To quantify the influence of variability, and in particular the distinction between individual (internal) variability and spatial environmental randomness, we measured its impact on the (quasi-)steady state particle density for both species. Figure 3(a) displays the relative change of the predator density $\rho_A(w_S, w_P)$ over the zero-variability case as a function of w_S and w_P for $\zeta = 0.3$. Both types of variability contribute additively and positively to the

density enhancement. Figure 3(b) shows the relative density change as a function of $w = w_S = w_P$ and ζ [32]. The prey density shows the same quantitative behavior for all parameter ranges. Hence we observe a significant increase of the population densities of *both* species for higher variability not only for purely spatial ($\zeta = 1$) randomness [5], but also for individual variability ($\zeta = 0$). In contrast, the effect of spatial randomness in either the prey birth rate σ or the predator death rate μ on the species densities stayed below a rather low value of 2%.

The striking minimum in the density increase occurring near a spatial influence factor $\zeta = 0.3$ arises from the combined variabilities through the quenched randomness of the lattice and the emergent variability of the individual particles. We argue that the density increase is primarily a monotonic function of the variability in the predation rate λ . Using the dependence of the predation rate λ on the spatial predation efficacy value η_S and the predation efficiencies of the participating particles η_A and η_B given in the text, the standard deviation of λ is $\sigma_\lambda = \sqrt{\zeta^2 \sigma_S^2 + (1 - \zeta)^2 (\sigma_A^2 + \sigma_B^2)}/2$. Due to the truncation of predation efficiency values to the range $[0, 1]$, the effective standard deviation of the spatial predation efficacy is different from the environmental variability parameter. Similarly, the standard deviation of the predation efficiencies of individual particles have to be taken from simulation data. Figure 3(c) shows the resulting standard deviation of λ as a function of w and ζ which is a measure of the effective combined variability. It reflects the minimum in the density increase at $\zeta \approx 0.3$. The data also emphasize that environmental variability has a more pronounced effect on the species densities as compared to demographic variability, since the density increase is disproportionately higher for $\zeta \rightarrow 1$.

Surprisingly, we observe that low individual variability with weak or no spatial influence, i.e. $0 < w_P \ll 1$ and $\zeta = 0$, yields the strongest species optimization with the maxima of the predator and prey populations closest to $\eta = 1$ and $\eta = 0$ respectively; see Fig. 1(a). But the enhancement of the overall species densities in this regime is minute and tends to zero for small w_P ; see the lower right corner of Fig. 3(b). The respective benefits of the up- / downward optimization of the predator / populations in terms of predation efficiency clearly almost cancel each other. Hence we conclude that predation efficiency optimization is essentially neutral and carries no benefit for either species in terms of their net population densities (at least in the context of our model), despite its vital necessity to ensure the survival of coevolving species. This also reinforces our argument that the density enhancement is a function of rate variability only.

The predator-predator and prey-prey correlation lengths l_{AA} and l_{BB} and typical predator-prey distance l_{AB} , measured by extracting the (quasi-)steady state exponential decay length and the position of the maximum (in the case of l_{AB}) from the correlation functions

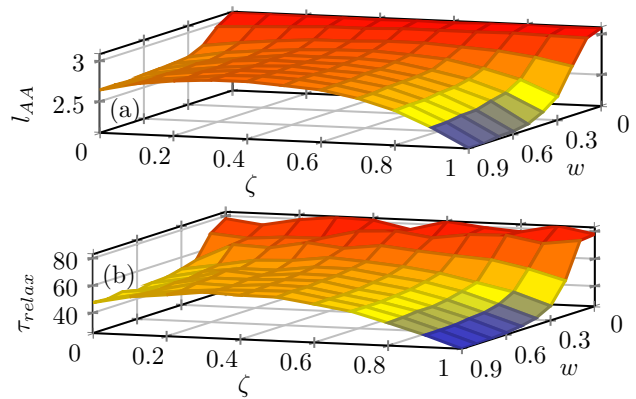


FIG. 4: (Color online.) (a) The correlation length l_{AA} from the predator-predator autocorrelation function. The prey-prey correlation length l_{BB} would essentially display the same shape as l_{AA} scaled by ~ 0.9 . (b) The predator density relaxation time τ_{relax} toward the quasi-stationary state.

$C_{\alpha\beta}(x) = \langle n_{\alpha i+x} n_{\beta i} \rangle - \rho_\alpha \rho_\beta$ with $\alpha, \beta = A, B$ [33], decrease for increasing variability w ; see Fig. 4(a). For $\zeta = 1$ we reproduce the data from Ref. [5], where we argued that the decrease in $l_{\alpha\beta}$ indicated a more tightly clustered population around lattice sites with small spatial predation efficiency η_S , leading to the observed enhanced densities and higher amplitudes in the initial population oscillations. Surprisingly we also see a (less pronounced) decrease of $l_{\alpha\beta}$ for $\zeta \rightarrow 0$, indicating the existence of spontaneously formed tight activity patches around clusters of highly optimized prey particles. To investigate the effect of the combined variability on the relaxation of the population densities we collected data on the characteristic decay time of the initial predator population oscillations by least-square fitting of an exponentially decaying sinusoidal function to the predator species density time series; see Fig. 4(b). As expected, increasing disorder w induces a roughly threefold decrease in the purely spatial case ($\zeta = 1$) and about a twofold decrease in the individual variability case ($\zeta = 0$).

In conclusion we performed an extensive numerical Monte Carlo simulation study to assess how external environmental randomness and individual variability modified through mutations during inheritance compete and affect the coevolutionary population dynamics of two co-existing species in a spatial stochastic LV model. The overall predator and prey densities are *both* enhanced by environmental variations, while evolutionary optimization within each species has an essentially neutral net effect. To better understand this evolutionary trait optimization, we derived a mean-field model that qualitatively reproduces our simulation results. In addition we find that increased individual variability stabilizes both populations against extinction. There are certainly other intriguing aspects pertaining to variability in ecological models that deserve further investigation, promising

amazingly rich features and crucial quantitative insight.

We gratefully acknowledge inspiring discussions with G. Daquila, E. Frey, J. Phillips, T. Platini, M. Pleimling, B. Schmittmann, and R.K.P. Zia.

* Electronic address: ulrich.dobramysl@vt.edu

† Electronic address: tauber@vt.edu

- [1] J. D. Murray, *Mathematical Biology*, 3rd ed., Vol. I and II (Springer, New York, 2002).
- [2] J. Hofbauer and K. Sigmund, *Evolutionary Games and Population Dynamics* (Cambridge University Press, Cambridge, 1998).
- [3] J. Smith, *Models in ecology* (Cambridge University Press, Cambridge, 1974) p. 145.
- [4] R. May, *Stability and complexity in model ecosystems*, Vol. 6 (Princeton University Press, Princeton, NJ, 1973).
- [5] U. Dobramysl and U. C. Täuber, Phys. Rev. Lett. **101**, 258102 (2008).
- [6] A. J. Lotka, J. Am. Chem. Soc. **42**, 1595 (1920).
- [7] V. Volterra, Mem. Accad. Sci. Lincei. **2**, 31 (1926).
- [8] A. Provata, G. Nicolis, and F. Baras, J. Chem. Phys. **110**, 8361 (1999).
- [9] A. Rozenfeld and E. Albano, Physica A **266**, 322 (1999).
- [10] A. Lipowski, Phys. Rev. E **60**, 5179 (1999).
- [11] M. Droz and A. Pekalski, Phys. Rev. E **63**, 051909 (2001).
- [12] T. Antal and M. Droz, Phys. Rev. E **63**, 056119 (2001).
- [13] M. Kowalik, A. Lipowski, and A. L. Ferreira, Phys. Rev. E **66**, 066107 (2002).
- [14] A. J. McKane and T. J. Newman, Phys. Rev. Lett. **94**, 218102 (2005).
- [15] H. Matsuda, N. Ogita, A. Sasaki, and K. Satō, Progr. Theoret. Phys. **88**, 1035 (1992).
- [16] J. E. Satulovsky and T. Tomé, Phys. Rev. E **49**, 5073 (1994).
- [17] N. Boccara, O. Roblin, and M. Roger, Phys. Rev. E **50**, 4531 (1994).
- [18] R. Durrett, SIAM Review **41**, 677 (1999).
- [19] M. Mobilia, I. T. Georgiev, and U. C. Täuber, Phys. Rev. E **73**, 040903(R) (2006).
- [20] M. Mobilia, I. T. Georgiev, and U. C. Täuber, J. Stat. Phys. **128**, 447 (2006).
- [21] M. J. Washenberger, M. Mobilia, and U. C. Täuber, J. Phys. Cond. Matter **19**, 065139 (2007).
- [22] A. Dobrinevski and E. Frey, Phys. Rev. E **85**, 051903 (2012).
- [23] T. Yoshida, L. E. Jones, S. P. Ellner, G. F. Fussmann, and N. G. Hairston, Nature **424**, 303 (2003).
- [24] O. Kishida, Y. Mizuta, and K. Nishimura, Ecology **87**, 1599 (2006).
- [25] J. S. Weitz, H. Hartman, and S. A. Levin, Proc. Natl. Acad. Sci. USA **102**, 9535 (2005).
- [26] T. Rogers, A. J. McKane, and A. G. Rossberg, Europhys. Lett. **97**, 40008 (2012).
- [27] A. Traulsen, J. C. Claussen, and C. Hauert, Phys. Rev. E **85**, 041901 (2012).
- [28] H. Fort and P. Inchausti, J. Stat. Mech. Theor. Exp. **2012**, P02013 (2012).
- [29] D. L. Hartl and A. G. Clark, *Principles of Population Genetics.*, 3rd ed. (Sinauer Associates, Sunderland, MA, 1997) Chap. 274-275.
- [30] More technical details about the algorithm can be found in Ref. [21].
- [31] For more details on the implementation of spatial variability see Ref. [5]
- [32] See Supplementary Material at URL for a spatial animation of a representative realization. The insert in the movie shows the temporal evolution of the population distributions.
- [33] Figs. 4-6 of Ref. [20] and Fig. 5 in Ref. [21] show these correlation functions for LV systems without disorder.